BOLLETTINO DI GEOFISICA TEORICA ED APPLICATA VOL. 42, N. 3-4, PP. 163-182; SEP.-DEC. 2001

Engineering implications of ground motions from the 1999 Turkey earthquakes

M. ÇELEBI

USGS, California, USA

(Received October 14, 2000; accepted August 7, 2001)

Abstract - The August 17, 1999 Izmit (Turkey) earthquake (M_w = 7.4) will be remembered as one of the largest earthquakes of recent times that affected a large urban environment. The shaking that caused the widespread damage and destruction was recorded by a handful of accelerographs operated by different networks in the earthquake area. As rebuilding in Turkey starts and picks up speed, the recorded ground motions that adversely affected the built-up environment are being studied intensively to explain the past disaster and for the implications for future earthquakes. New forecasts of future large earthquakes in the ever growing urban environment of Istanbul and its vicinities necessitates better preparation and extensive planning to upgrade and retrofit existing infrastructures. To successfully execute these endeavors, it is imperative to have better defined ground motion characteristics. This paper aims at discussing the issues related to the engineering implications of the recorded ground motions. The main shock records show that the peak accelerations, even those from near-field stations that exhibit the characteristic near-fault pulses that cause large displacements, are smaller than expected. On the other hand, smaller magnitude aftershocks yielded larger peak accelerations. This is attributed to the sparse networks, which possibly missed the recording of larger motions during the main shock - particularly in the heavily damaged areas of South Izmit Bay. Aftershocks recorded at such areas are used to estimate the missed main shock ground motions. Accordingly, the estimated motions in South Izmit Bay are approximately 1 g highly polarized in N-S direction. These attributes have significant engineering implications to be considered during the rebuilding phase and beyond.

Corresponding author: Mehmet Çelebi, USGS (MS977), 345 Middlefield Road, Menlo Park, CA 94025; phone: 650 329 5623; fax: 650 329 5163; e-mail: celebi@usgs.gov

1. Introduction

It is now well known that improper design and construction practices played an important role in the detrimental performance of more than 20,000 structures during the August 17, 1999 (M_w = 7.4) Izmit earthquake. This being a given part, the main goal must be to improve design and construction practices. During this process, it is important to assess the recorded ground motions, site effects and other earthquake related hazard issues which need to be considered during rebuilding efforts. (U.S. Geological Survey, 1999).

On-scale recordings of ground shaking during earthquakes are important to understand the causes of earthquake damage and the physics of fault rupture, and to advance design codes. Approximately 38 strong motion ground records were made of the August 17, 1999 Izmit earthquake by different institutions in Turkey that operate strong motion networks.

The purposes of this paper are to (a) discuss the characteristics and engineering implications of the strong-motion records of the Izmit, Turkey earthquake, (b) relate them to experiences elsewhere, (c) deliberate on pragmatic applications in Turkey for assistance in rebuilding, and (d) identify issues that must be dealt with before the next earthquake strikes the area.

2. Strong-motion records

2.1. The networks and recorded accelerations

The National Strong-Motion Network of the earthquake Research Department of the Ministry of Public Works (NSMN-ERD), the largest strong-motion network operator in Turkey, is aiming to deploy one strong-motion instrument in every major town within the earthquake zones of Turkey. This systematic effort by NSMN-ERD, supplemented by strong motion stations deployed by Kandilli Observatory and the Earthquake Research Institute (KOERI) and Istanbul Technical University (ITU) in Istanbul and the Marmara Region produced very significant and important records that will be useful for studying the earthquake and establishing important and necessary criteria in rebuilding efforts. These organizations recorded the main shock at approximately 38 stations within the epicentral region. Peak accelerations of the records from some of the stations are plotted into the map in Fig. 1. To date, detailed site characterizations of these stations have not been documented.

The current strong-motion network in the epicentral area (and in other segments of the North Anatolian Fault and elsewhere in Turkey, for that matter) is quite sparse. Therefore, it is important to consider that recording of larger peak accelerations might have been missed. For example, no record of the main-shock was obtained in Gölcük and vicinity in the immediate epicentral area - where there was extensive damage. Hence, absence of strong-shaking records inhibits a reliable evaluation of the effect of the shaking and ensuing damage on the typical structures in the area. In addition, only one record (minus a component due to malfunction) was retrieved from Adapazari, at station SKR, which was on stiff soil in the undamaged part of Adapazari.

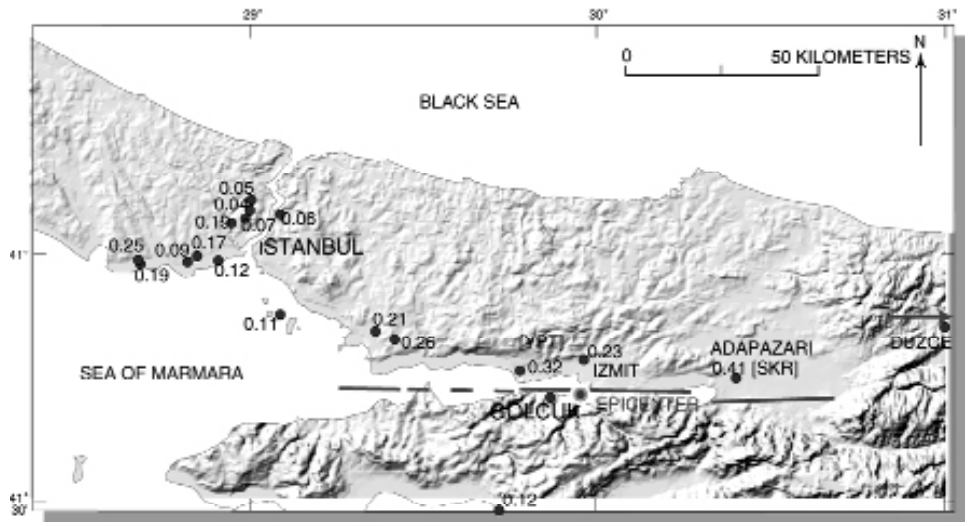

Fig. 1 - Map showing significant peak accelerations in the earthquake affected area, plotted at relative locations of significant strong-motion stations within and in close proximity to the epicentral area (Base map courtesy of BKS Surveys Ltd., N. Ireland). Approximate fault rupture trace is also shown. Stations YPT and SKR are two significant referenced stations.

There were no permanent stations in the fast-growing urban/industrial areas of the Adapazari basin (east of Adapazari). The peak accelerations in the basin, almost certainly were amplified compared to that recorded at the stiff soil site. The shaking in the basin would also probably have revealed different characteristics such as amplification due to softer layered media, basin effects and in certain areas, the effect of liquefaction that occurred.

Therefore, during the main shock of the August 17, 1999 earthquake, the largest recorded peak accelerations (SKR, 0.41 g horizontal and Düzce, 0.48 g vertical) were most likely not the largest that actually occurred. This possibility is strengthened by the fact that accelerations with larger peaks were recorded during events of smaller magnitudes. This is illustrated in Fig. 2

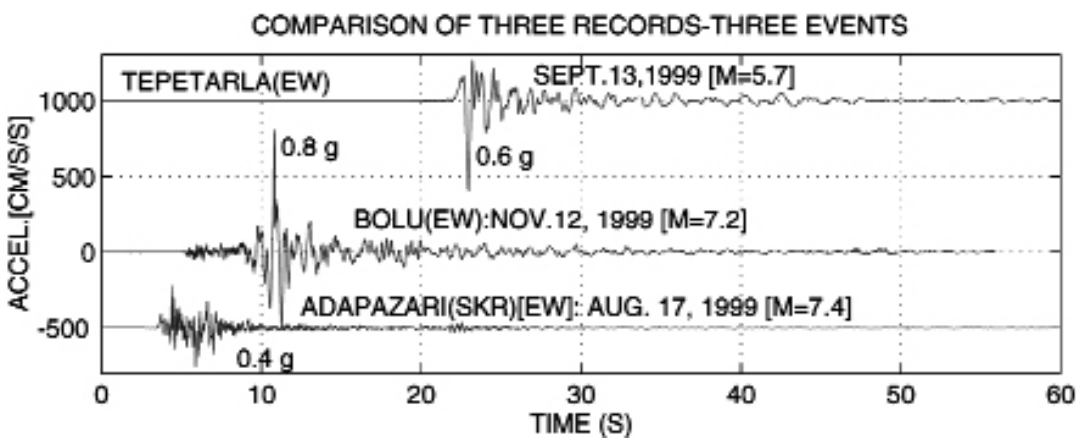

Fig. 2 - Comparison of peak accelerations for the August 17, 1999 main shock (station SKR) and two aftershocks, each recorded at a different location.

which shows three acceleration time-histories recorded during: (a) the M_s = 5.7 aftershock on 13 September 1999 at Tepetarla (a temporary station near Izmit) with peak ~ 0.6 g, larger than any peak recorded during the main shock, for example, (b) the SKR record, and (c) the November 12, 1999 (M_s = 7.2) Düzce event, station (Bolu) with peak ~ 0.8 g (EW).

Two samples of recorded main shock motions are presented. Fig. 3a shows 40 s of the acceleration time-histories recorded at SKR (Adapazari in Sakarya Province) on stiff soil. The records exhibit more than three different shocks. Fig. 3b shows the time variant sum of the

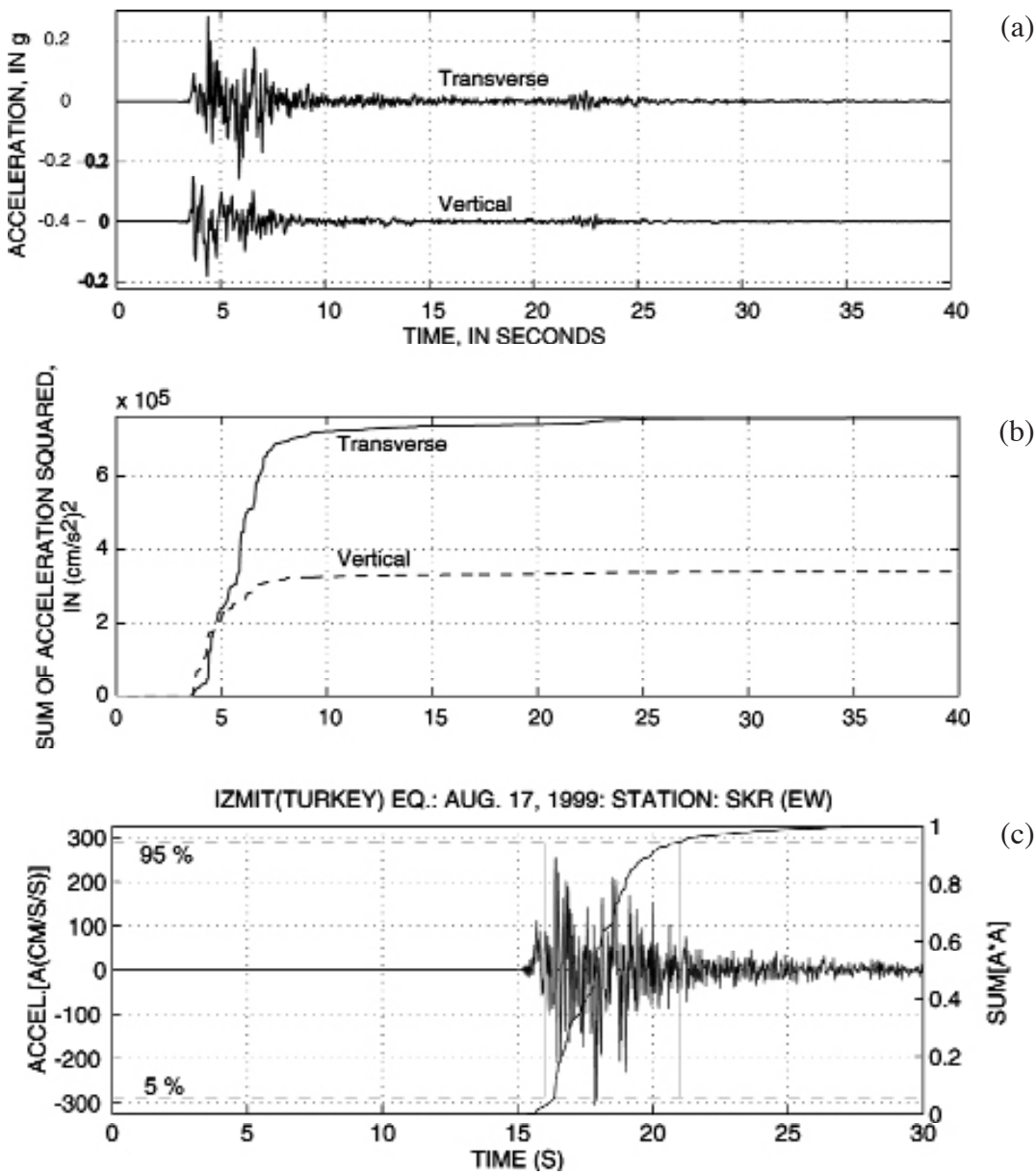

Fig. 3 - 40 s window of the (a) SKR record time history and (b) cumulative squared acceleration. (c) Definition of duration of strong shaking (time between 5-95% of the relative cumulative squared acceleration; Novikava and Trifunac, 1994), for the transverse component.

square of the acceleration to depict relative cumulative significant shaking (representative of energy). As depicted in Fig. 3c, the duration of strong shaking is determined as approximately 5 seconds, using the time span between 5%-95% of the normalized sums (Novikava and Trifunac, 1994). The main shock contributes to approximately 70% of the total significant shaking of the two shocks within the 40 seconds of the record.

In Fig. 4, the acceleration time-history of YPT (Petro-Chemical Plant in Körfez) is shown. The site is alluvial. The figure exhibits two distinctive earthquakes. The figure also shows the relative cumulative significant shaking as calculated by summing the square of the acceleration over time. This figure shows that the strong shaking of the earthquake lasted approximately 5-6 seconds.

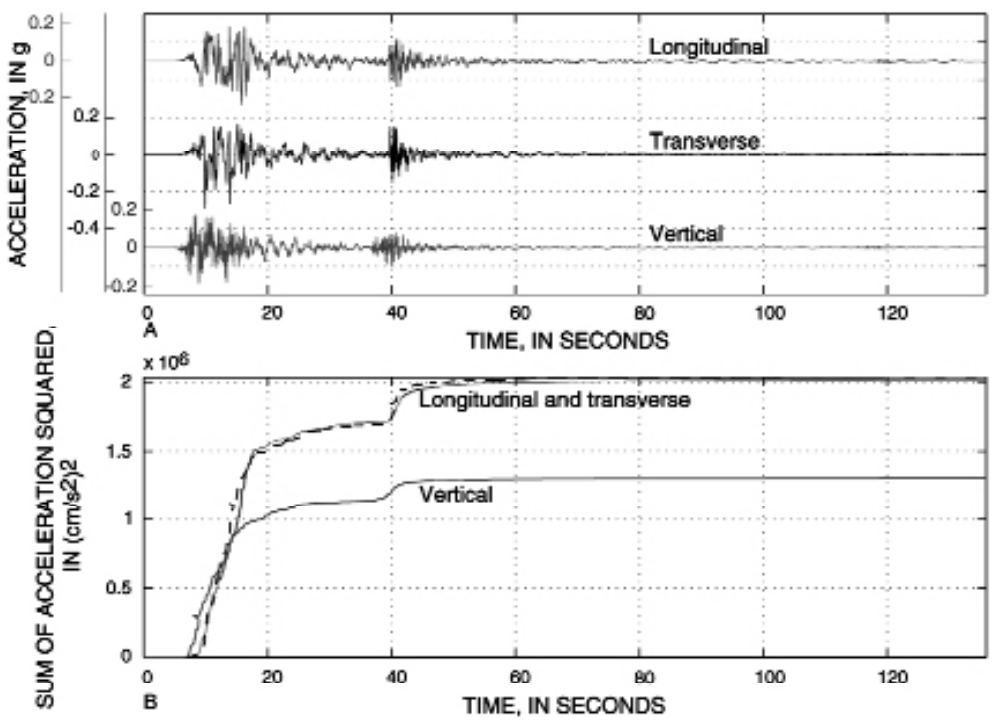

Fig. 4 - Time-history of YPT. The plot shows the second event approximately 30-seconds after the first (top) and the significant strong shaking of the mainshock contributes for approximately 70 % of the total and the strong shaking duration is 5-6 s (bottom).

2.2. Near-fault issues and pulses

Abrahamson (2000) recently noted that, on a worldwide scale, there were only 8 records within < 20 km from the fault for M > 7 earthquakes between 1940 and 1999. The 1999 in earthquakes Turkey and the Chi-Chi, Taiwan earthquake of September 21, 1999, respectively added 5 and 60 more records to a total of 73. One of the main reasons why near-fault motions are important is the presence of long-duration pulses that result in large displacements, which are detrimental to the performance of long-period structures.

Somerville (1998) explains the long-period pulse characteristics of near-fault motions as follows:

- the propagation of fault rupture toward a site at a velocity close the shear wave velocity causes most of the seismic energy from the rupture to arrive in a single large long-period pulse of motion;
- the pulse of motion represents the cumulative effect of almost all of the seismic radiation from the fault, and
- the radiation pattern of the shear dislocation on the fault causes this large pulse of motion to be oriented in the direction perpendicular to the fault, causing the fault-normal peak velocity to be larger than strike-parallel peak velocity.

Since long-duration pulses translate into large displacements, a simple explanation using vibrational physics of pulse action is useful for developing a simple and quick assessment and demonstration tool of such actions. Consider four undamped, single-cycle sinusoidal accelerations with equal amplitudes, $\ddot{Y}$, but having different pulse durations. Fig. 5 shows that corresponding displacements, y, are increased with the increase in pulse duration, T_p, by virtue of the relationship: $y = -\ddot{Y}/(2\pi / T_p)^2$. It should be remembered that the amplitude to be considered is the amplitude of the pulse with the longest cyclic period and not necessarily the peak amplitude of the time-history of a record which may occur at an higher frequency cycle. Also, in using the simple process for integration, it is assumed that the accelerogram is a continuous sinusoid and not a truncated sinusoid.

This grossly simplified visualization of the effect of long-period pulses in generating large pulse displacements are quantified and verified for three different earthquake records. The YPT record seen in Fig. 4 is re-plotted in Fig. 6 to better exhibit the long-period pulses and the amplitude spectra with a pulse period (T_p) of about 5 s (0.2 Hz) for the horizontal components. With peak acceleration of 0.22g for the EW component, the calculated pulse displacement, $y = 0.22 \cdot 981 / (2\pi / 5)^2 \sim 137$ cm. compares well with the displacement obtained by double-integration (Fig. 7). This and two other examples are summarized in Table 1. Fig. 8 shows three components of accelerations recorded at Station TCU068 during the (M = 7.3) September 21, 1999 Chi-chi (Taiwan) earthquake and their amplitude spectra that exhibit the lowest dominant frequency of approximately 0.11 Hz ($T_p \sim 9.09$ s). With a peak acceleration of 0.51 g for the east-west component, the peak pulse displacement of 1027 cm is calculated. This compares well with the displacement of 707 cm (Fig. 9) obtained by double integration of the accelera-

Table 1 - Evaluation of peak displacements using sinusoidal pulse analogy versus double integration of recorded acceleration.

Earthquake	Mag. M_w	Station	Peak Acc. [g]	Pulse		Sinusoidal Pulse Displ. [cm]	Integrated Displ. [cm]
				f (Hz)	T_p (s)		
Izmit [Turkey] 1999	7.4	YPT [EW]	0.22	0.2	5.0	137	~175
Chi-chi [Taiwan] 1999	7.6	TCU068 [EW]	0.51	0.11	9.09	1027	707
Erzincan [Turkey] 1992	5.8	ERZ	0.5	0.5	2.0	50	35-70

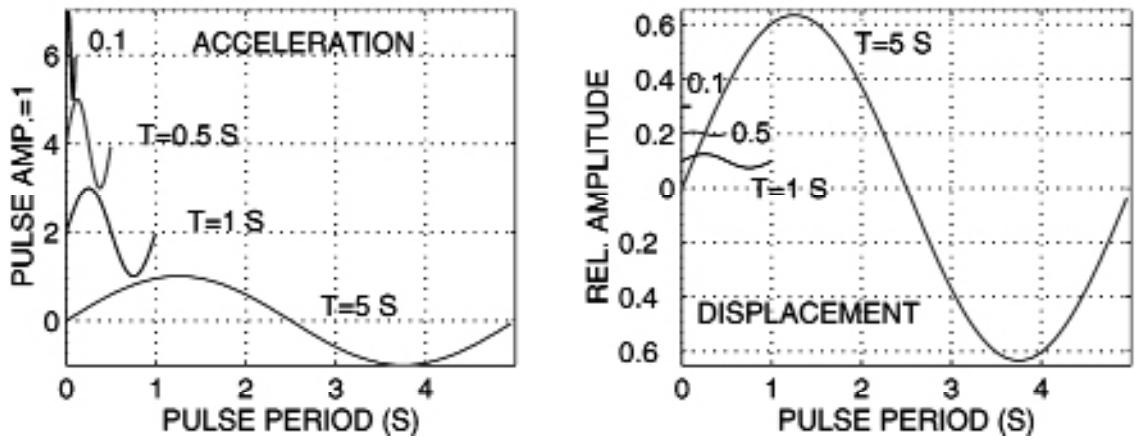

Fig. 5 - Single-cycle sinusoidal accelerations with constant amplitude but varying periods and corresponding displacements.

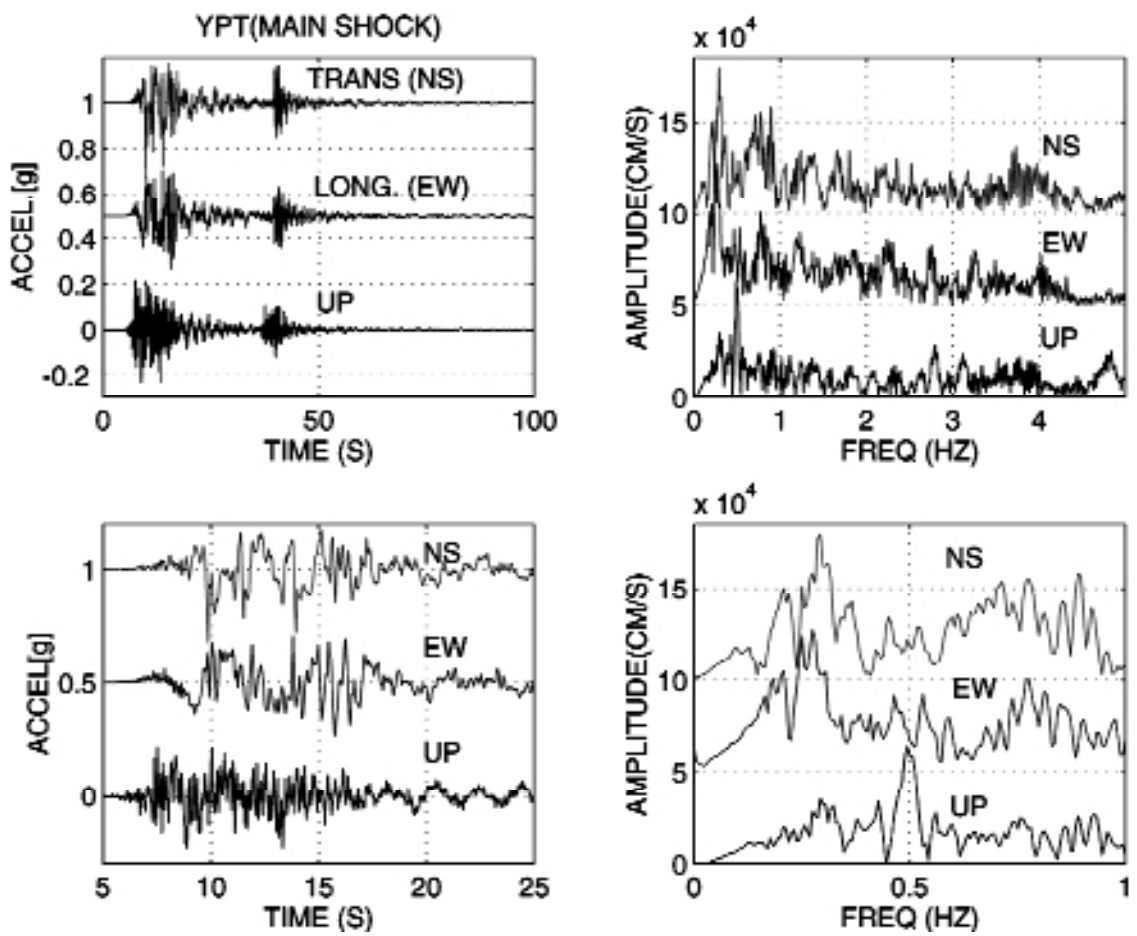

Fig. 6 - The three components of the main-shock motions at YPT (Yarimca) recorded during the 19 August Izmit earthquake. The amplitude spectra of the motions are also shown.

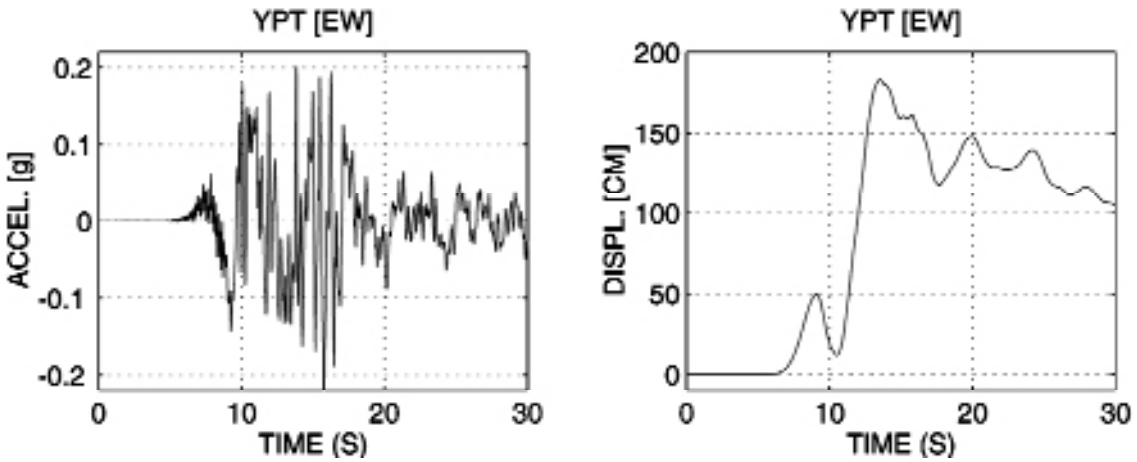

Fig. 7 - Recorded E-W component of acceleration and integrated velocity and double-integrated displacements at YPT.

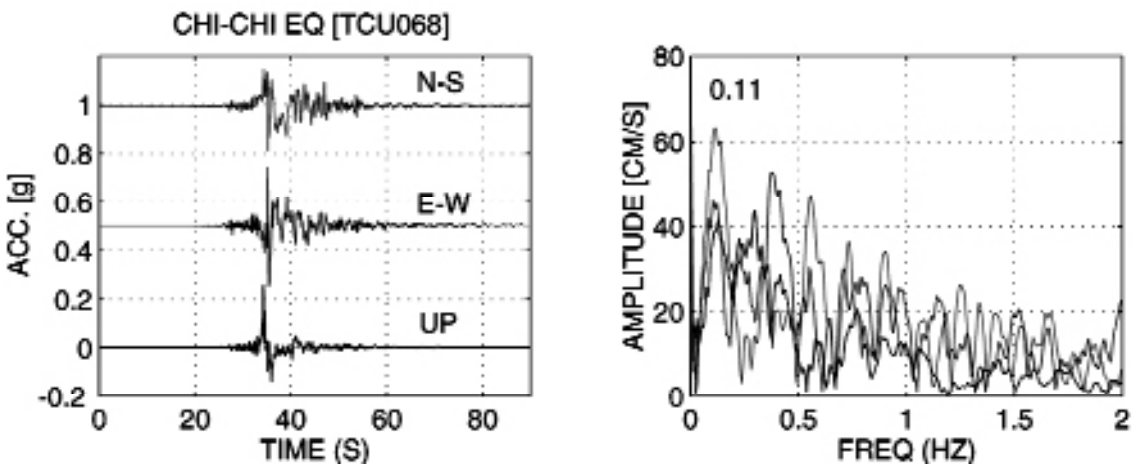

Fig. 8 - Accelerations recorded at the TCU068 Station during the Chi-Chi (Taiwan) earthquake and the amplitude spectra (data from Lee et al., 1999).

tion record (Tsai, 2000). The third example is the 13 March 1992 Erzincan earthquake record (Fig. 10). Accepting the $T_p \sim 2$ seconds and the peak acceleration as approximately 0.5 g, then the estimated displacement is ~ 50 cm. The margin of variation of peak accelerations provides the calculated displacement variation of 35-70 cm.

Thus, since long-period acceleration pulses result in higher velocities and displacements, it is important to assess how the large displacements affect the response and performance of long-period structures such as tall buildings, long-spanning bridges, viaducts, overpasses, and base-isolated structures.

Consequently, to compensate for the additional demand in design strength caused by such large displacements, recent codes in the United States adopted the Near Fault Factors (Uniform Building Code, 1997). Thus, the seismic zoning factors are effectively increased by a factor,

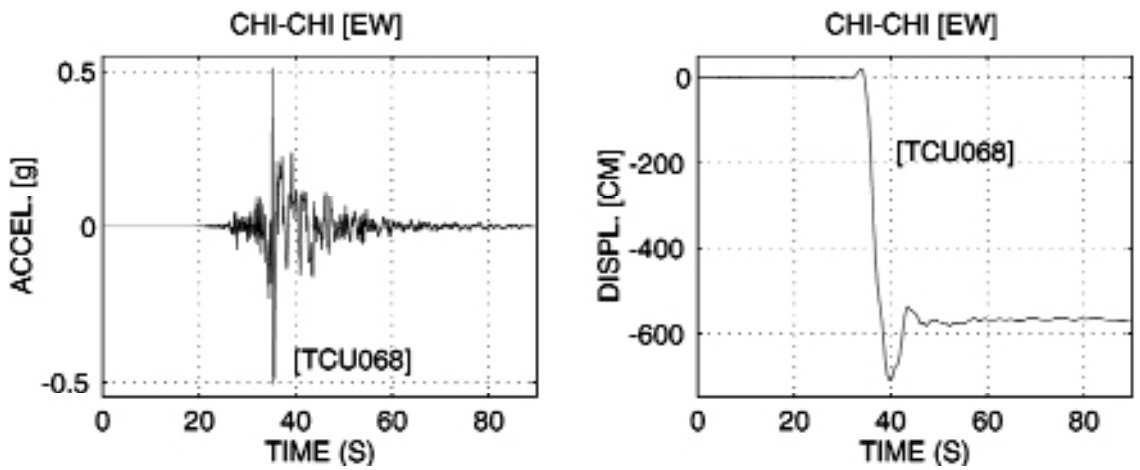

Fig. 9 - Recorded acceleration and integrated displacement of TCU068 station E-W component (from Boore, 2000).

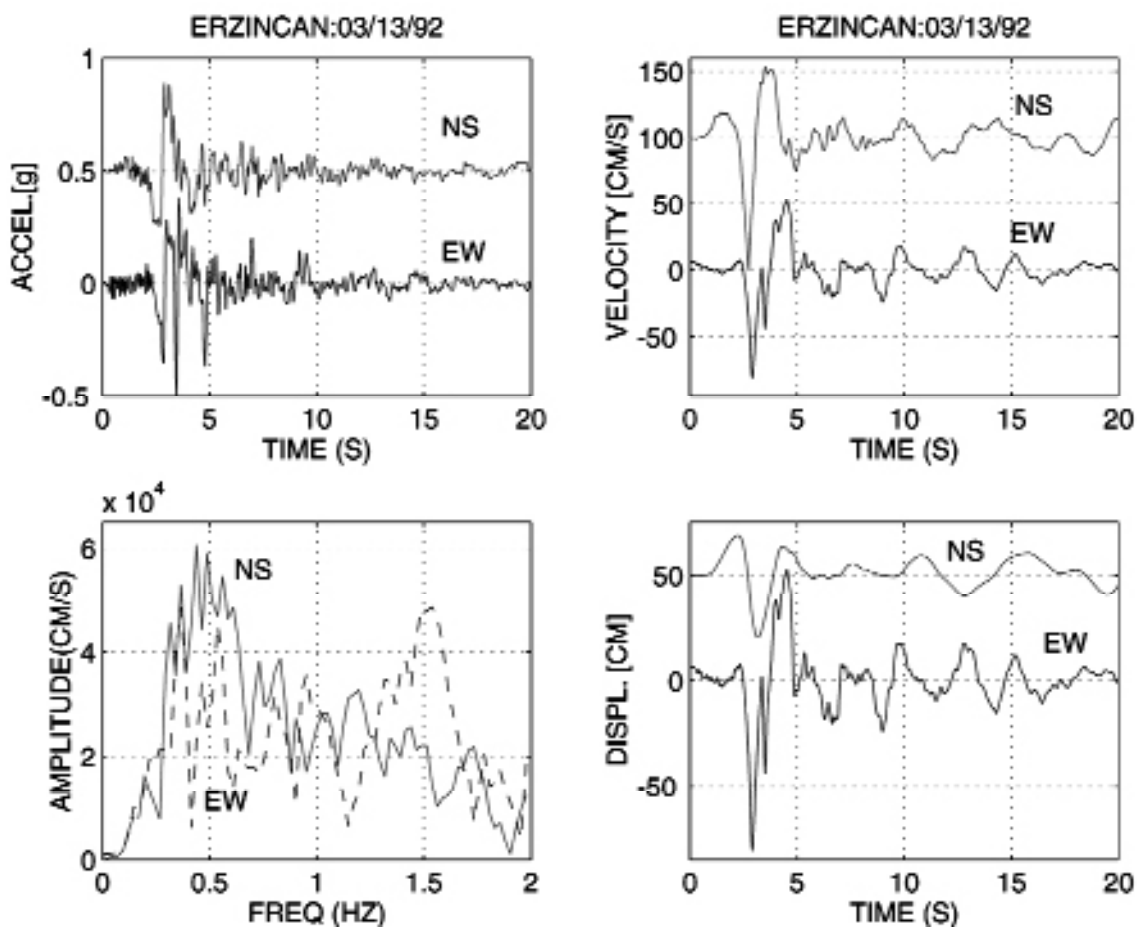

Fig. 10 - The N-S and E-W (acceleration, velocity and displacement) components of the 1992 Erzincan record (note: the lowest dominant frequency of the acceleration record is ~ 0.5Hz).

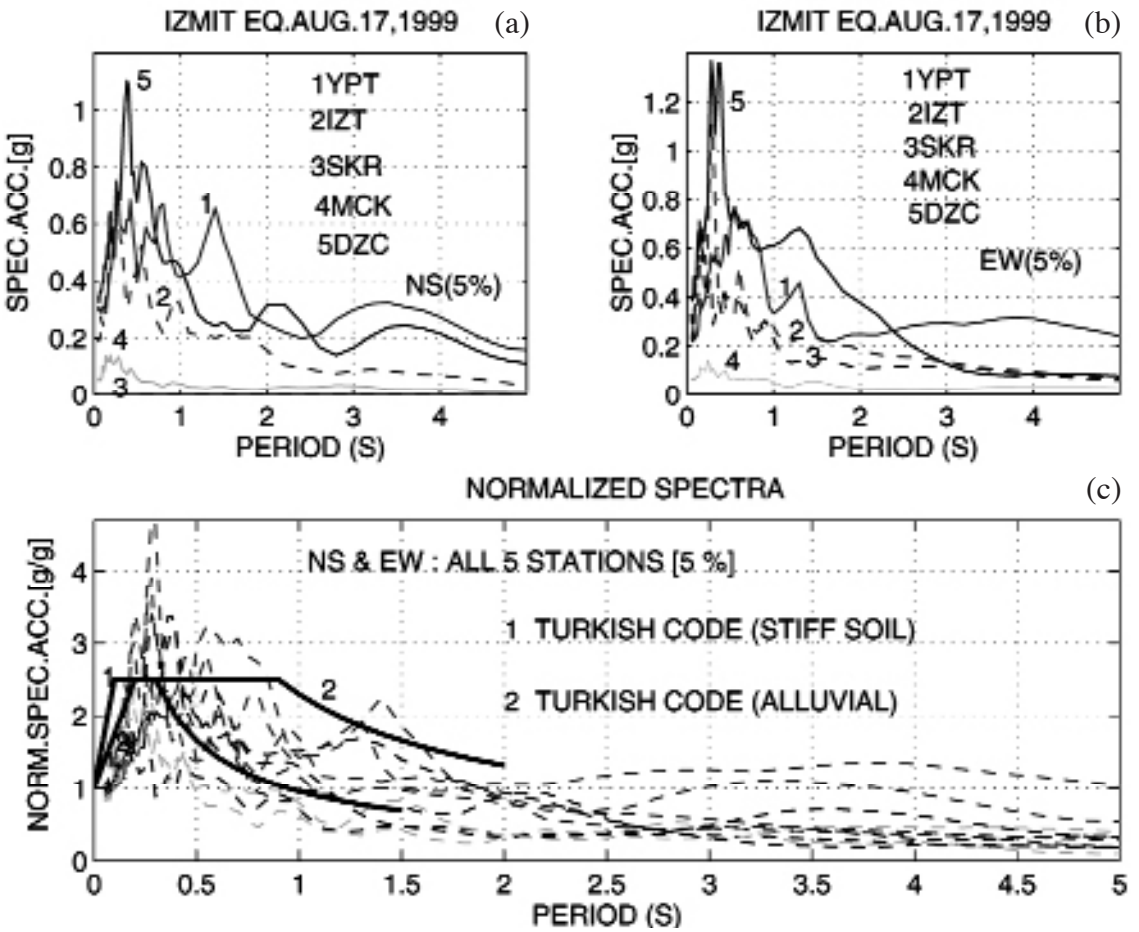

Fig. 11 - Response spectra (5 % damped) for 5 stations (a and b) and (c) normalized response spectra of 5 stations compared with design response spectra of Turkish Code (Specifications, 1998).

$1 < N < 2$ for seismic zone 4 (the highest seismic risk zones in the United States) within 10 km of those fault zones that are capable of generating (a) $M \geq 7$ earthquakes with slip rates exceeding 5 mm/year or (b) earthquakes $M \geq 6.5$ with slip rates smaller than 5 mm/year[1]. The North Anatolian Fault (NAF) is tectonically similar to the San Andreas Fault in

[1] In the Uniform Building Code, the total design base shear in a given direction is determined from the following formula: $V = (C_v I / R\ T)\ W$, where C_v is the seismic coefficient (for zone 4, it is given by $0.32\ N_v$, $0.40\ N_v$, $0.56\ N_v$, $0.64\ N_v$, $0.96\ N_v$ for soil profile types S_A (shear wave velocity, $V_s > 1500$ m/s), S_B ($760 < V_s < 1500$ m/s), S_C ($360 < V_s < 1500$ m/s), S_D ($180 < V_s < 360$ m/s) and S_E ($V_s < 180$ m/s), respectively), I is the importance factor, R is the ductility factor, T is the fundamental period of the design structure and W is the weight of the structure. The total design base shear V_d is not to exceed $(2.5\ C_a\ I / R)\ W$ but should not be less than $V = (0.11 C_a I\ W)$ where C_a is the seismic coefficient and similarly ranges as $0.32\ N_a$, $0.40\ N_a$, $0.40\ N_a$, $0.44\ N_a$ and $0.36\ N_a$ for the soil profiles S_A, S_B, S_C, S_D and S_E respectively. Furthermore, for Seismic Zone 4, the total base shear shall also be not less than the following: $V_d = (0.8\ ZN_v\ I / R)\ W$. Z is the seismic zone factor and is 0.4 for zone 4. In the above, $1 < N_v < 2$ and $1 < N_a < 1.5$ and are interpolated from tables according to the different type of soil profiles and distance from the fault. The highest factors are for sites less than 2 km from the faults (Uniform Building Code, 1997).

California; therefore, such factors should also be considered in selective zones along the NAF. The recorded responses clearly show long period pulses (e.g. ~ 5 s in case of YPT record - Fig. 6).

2.3. Response spectra

Figs. 11a-c show the response spectra and the normalized response spectra (all calculated for 5% damping), for north-south and east-west directions, respectively, for five stations, including the two (SKR and YPT) for which the time-history plots have been presented (Figs. 2-3). These five stations cover the epicentral area (stations IZT and YPT) and locations that are heavily damaged east of the epicentral area (SKR and DZC) and a location in Istanbul (MCK). IZT, YPT and DZC are on alluvial sites, whereas SKR and MCK are on stiff soil and rock, respectively. The response spectra show that the resonant periods (frequencies) change drastically at different stations. Furthermore, the normalized response spectra indicate that both YPT and DZC have long periods (low frequencies). For comparison of response spectra shapes, Fig. 10c also shows the current Turkish Code response spectra for stiff soil and alluvial site conditions (specifications for structures to be built in disaster areas; Ministry of Public Works and Settlement Government of Republic of Turkey, 1998). The figure indicates that for periods between 0.1-1, the design response spectra, similar to those used in the United States, are changed for this earthquake.

Taller buildings on the rocky hills of Istanbul, and the two suspension bridges in Istanbul were not adversely affected by the long-period motions of this earthquake - most likely due to attenuated ground motions. However, the important lifeline structures need to be reviewed for an earthquake that might occur closer to Istanbul.

3. Aftershock deployments and site response issue

Since the strong-motion network in the epicentral area of the Izmit earthquake was not dense enough to define ground shaking at all damaged areas, a limited number of temporary arrays were deployed to obtain aftershock records to explain site effects at various locations. USGS deployed a number of acceleration and velocity transducers at the South Izmit Bay including Gölcük. Fig. 12a-b shows the deployment of the temporary array in Gölcük and a set of seismograms of an aftershock obtained from both sides of the observed normal fault scarp that occurred during the main event. Stations FOC and GEM are on the hanging wall and LOJ and GYM are on the footwall of the normal fault. The figure exhibits the variation of ground motion at locations that are short distances apart (<1 km) (Çelebi and Sekiguichi, 2000) as well as the motions on both sides of the normal fault scarp. The differences of motions on either side of the normal fault are also observed in Fig. 12c-d. The amplitude spectra and the relative cumulative energy plots further reinforce the higher energy at FOC and GEM, on the hanging wall as compared to LOJ and GYM, on the footwall.

Aftershock data from Gölcük and other parts of the south Izmit Bay are compiled separately (Çelebi et al., 2001) and are being studied in detail to estimate main shock ground motion at significant locations of the South Izmit Bay (Çelebi and Sekiguichi, 2001).

Fig. 13 shows the mean transfer functions of 11 events for FOC and LOJ, calculated using Nakamura's method (1989, 2000) which, in absence of reference rock sites, facilitates calculation of a transfer function as a ratio of amplitude spectra of horizontal to vertical components of motion at a station [$R = A$(horizontal) /A(vertical)]. For frequencies of less than 2 Hz, the north-south components exhibit almost twice the amplification at FOC when compared

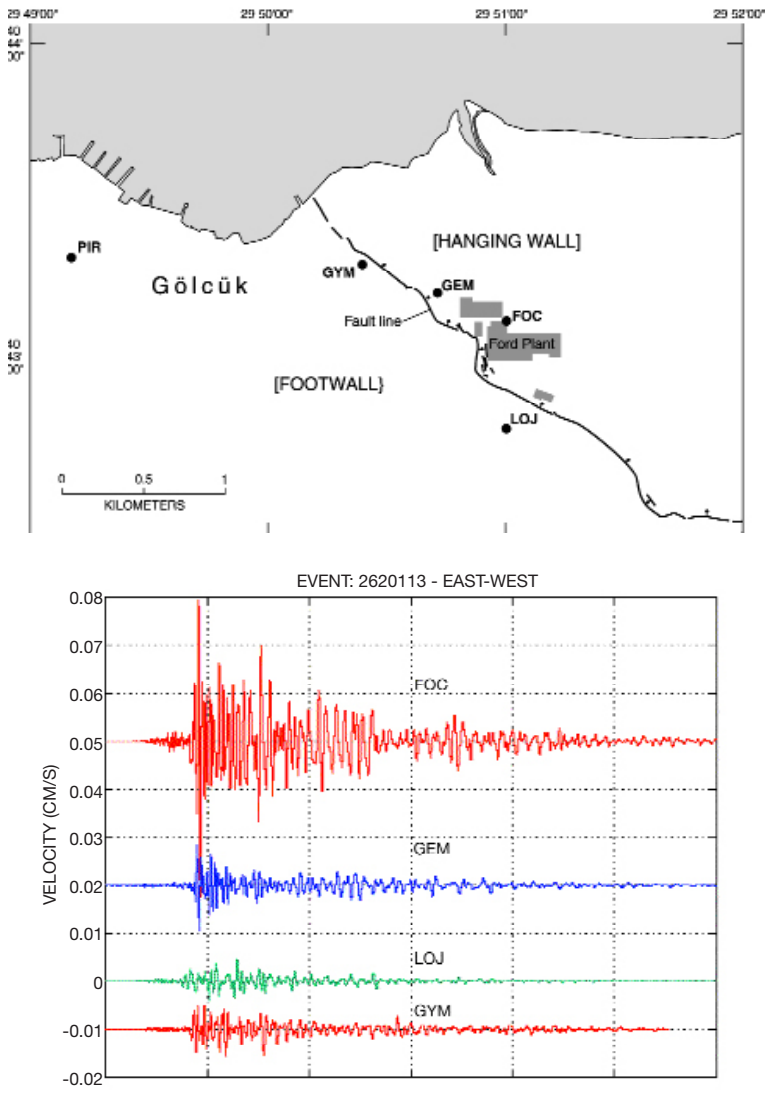

Fig. 12 - Aftershock deployment in Gölcük (a), (b) seismograms, (c) relative cumulative energy, and (d) normalized amplitude spectra from an aftershock. The seismograms show relative amplitudes of velocity records at close distances (<1km). The stations FOC, GEM and LOJ are within the Ford Plant Grounds near Gölcük. Station GYM is within <1 km to these stations. The relative cumulative energy plots of one event exhibiting significant difference of energy on either side of the vertical faulting.

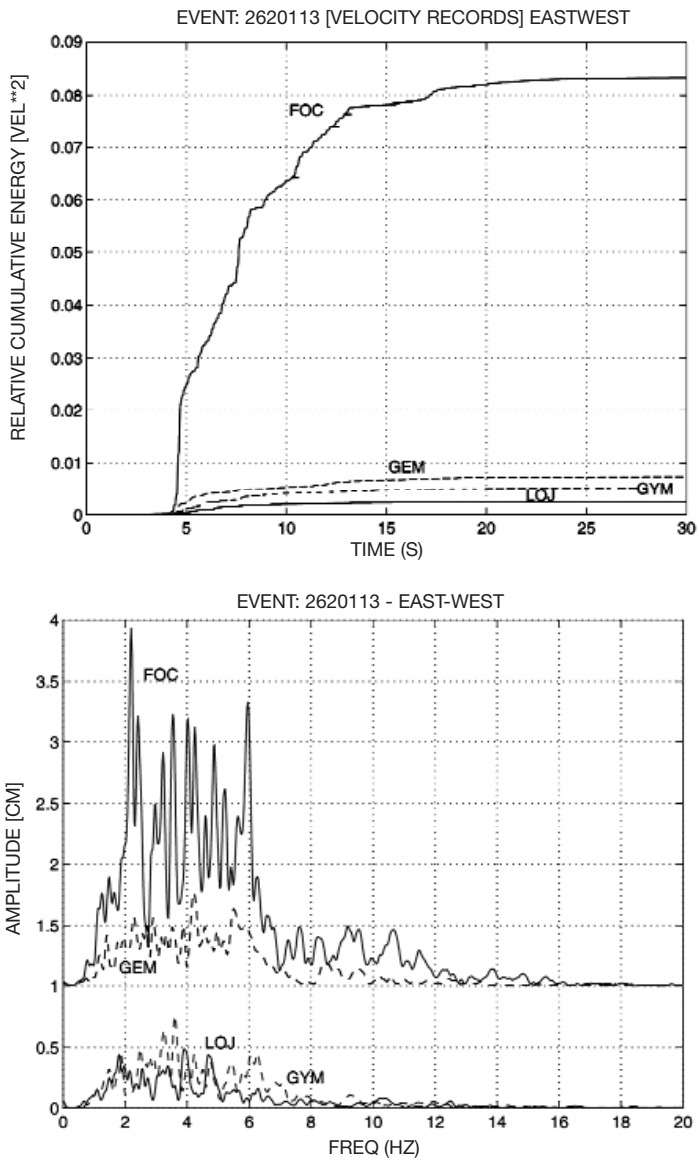

Fig. 12 - continued.

to LOJ. This implies that in the hanging wall, alluvial deposits are deeper. This is substantiated by the fact that, historically, there have been similar earthquakes in the area approximately every 250 years (e.g. two prior earthquakes, now confirmed by geological trenching and carbon dating, occurred in 1719 and 1509 AD, respectively (Barka, 2000; Sieh, 2000). Thus, over the centuries, repetitive hanging walls have been filled over with alluvial material. Identification and recognition of such fault locations with associated historical events is necessary for siting purposes of facilities and important infrastructures in such areas.

The aftershock data are also used to estimate the strong-motions during the main event. Fig. 14 shows the estimated motions for FOC using aftershock data at both FOC and YP1 (same as YPT in Fig. 1) and the recorded mainshock data at YPT (Çelebi and Sekiguchi, 2000). The

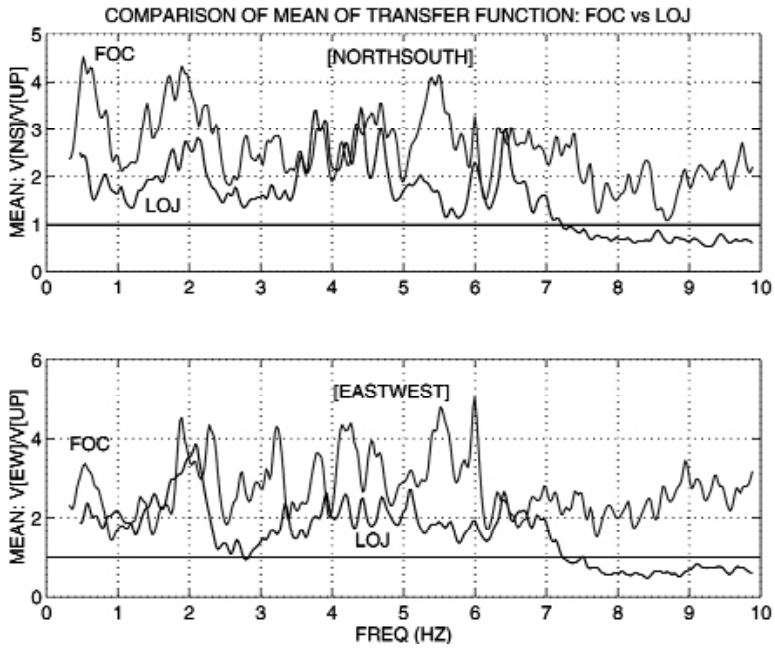

Fig. 13 - Mean transfer function of 11 events showing the amplification differences on both sides of the vertical faul-

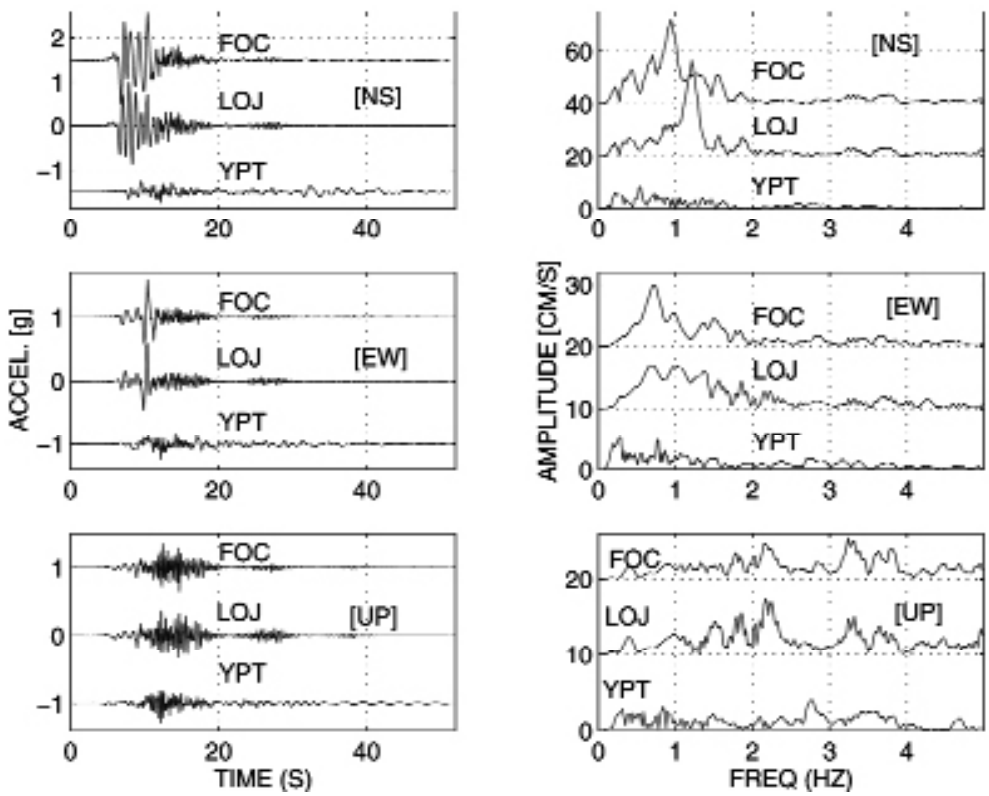

Fig. 14 - Estimated (main-shock) ground motions and respective amplitude spectra at FOC and LOJ using inversion technique with aftershock recordings at FOC and YP1 (from Çelebi and Sekiguchi, 2000). Note the fault-normal motions are larger for both FOC and LOJ.

process termed as inversion uses (a) simulated ground motion in the lower frequency range (0.1-1.5 Hz) by Green's theoretical functions for a laterally homogeneous structure model and a source process model obtained by Sekiguchi and Iwata (2000), (b) stochastic Green's function (Boore, 1983) for the higher frequency range (1.5-10 Hz). Simulated ground motion at the FOC station (Fig. 14) is highly polarized to NS component, the fault normal direction. These characteristics have been observed at stations in source regions of past earthquakes. Therefore, it is important to consider directivity effects of near-fault ground motions, as also stated by Somerville (1998).

4. Other issues

4.1. Soil-structure interaction

The majority of the building inventory on alluvium media were most likely subjected to soil-structure interaction effects (SSI). The foundations of the buildings with 1-8 stories had very small or no embedment. Most were constructed on continuous beam foundations. SSI is particularly important for those structures that had little or no embedment (D) as compared to the height (H) or width (L) of a building ($0 < D/H < 0.5$). Aviles and Perez-Rocha (1998) recently showed (Fig. 15) that the effective period of structures can increase by a factor of 2 for $H/L \sim 3$. In this figure, accepting $T_h = H/(V_s T)$ as relative measure of relative stiffness of the structure to that of the soil, T_h can be approximated as $T_h \sim 30/V_s$ (for an average 3 m height per story and $T \sim 0.1N$, (N number of stories) for most structures. V_s, in general, is the shear wave velocity of the uppermost 30 m of the soil. For $V_s = 300$, $T_h \sim 0.1$ and for softer soils with $V_s = 60$ m/s, $T_h \sim 0.5$. The shifting of the resonant period due to SSI may adversely affect the performance of structures by shifting the fundamental period to a longer value; thereby

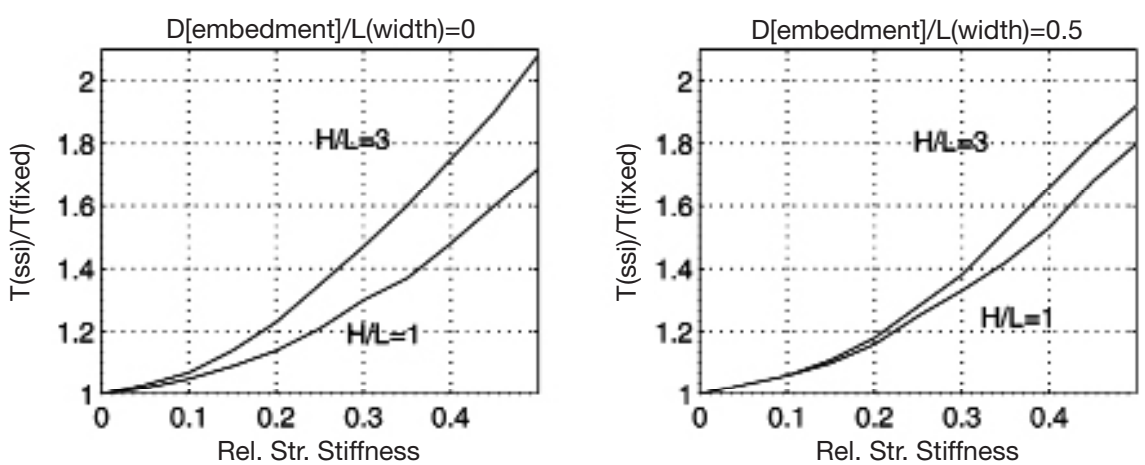

Fig. 15 - Effect of foundation embedment on structural period when soil-structure interaction is included (redrawn from Aviles and Perez-Rocha, 1998).

enhancing the effects of long-period ground motions. In rebuilding, embedment and foundation issues must be addressed.

4.2. Implications for the future

Finally, an issue that needs to be addressed is the future forecasting following the 17 August 1999 earthquake. Parsons et al. (2000) forecasted that the August event increased the stress in the Marmara Sea toward Istanbul, the largest city in Turkey (Fig. 16). They forecast that the stress increase results in the probability of 62 ± 15% for a M > 7 an earthquake occuring in the next 30 years. Thus, there is an urgent need to be ready.

4.3. Fault rupture zoning and implications for Turkey

The experiences in California, USA, related to fault rupture zones, is particularly appropriate for Turkey too. The NAF and San Andreas Faults are both right-lateral strike slip faults, they have similar lengths (~1500 km) and produce significant earthquakes.

In 1972, following the 1971 San Fernando earthquake in California, the California State Assembly passed the Alquist-Priolo Earthquake Fault Zoning Act. The purpose of the law was

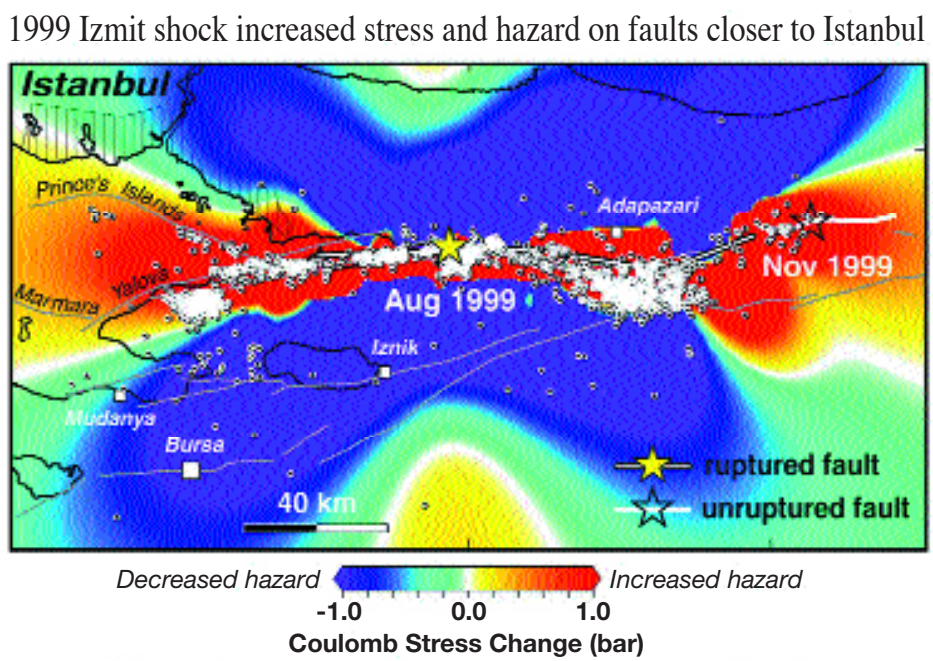

Fig. 16 - Change in stress pattern triggered by the Izmit earthquake on 17 August 1999 (courtesy of R. Stein). Yellow to red colors indicate the area where stress increased, whereas the green to purple colors show the area where the stress decreased in the wake of the Izmit event (Parsons et al., 2000).

to prevent construction on or near the surface fault rupture zones. It led to the establishment of offset distances from the surface fault rupture zones. During the 17 August 1999 earthquake, numerous buildings and industrial plants were adversely affected because they were on or near the fault surface rupture zones. Turkey must establish such zones, to be used by municipalities and provinces, to prevent construction within the fault zones. A sample fault zone map is shown in Fig. 17. The Alquist Priolo Act is provided in Appendix A.

In 1990, in California, another significant act, the Seismic Hazards Mapping Act was adopted. The important aspect of this act is summarized in this quotation: "The Legislature finds and declares all of the following:

1. the effects of strong ground shaking, liquefaction, landslides, or other ground failure account for approximately 95 percent of economic losses caused by an earthquake;
2. areas subject to these processes during an earthquake have not been identified or mapped statewide, despite the fact that scientific techniques are available to do so;
3. it is necessary to identify and map seismic hazard zones in order for cities and counties to adequately prepare the safety element of their general plans and to encourage land use management policies and regulations to reduce and mitigate those hazards to protect public health and safety". Fig. 18 shows a sample seismic hazard map.

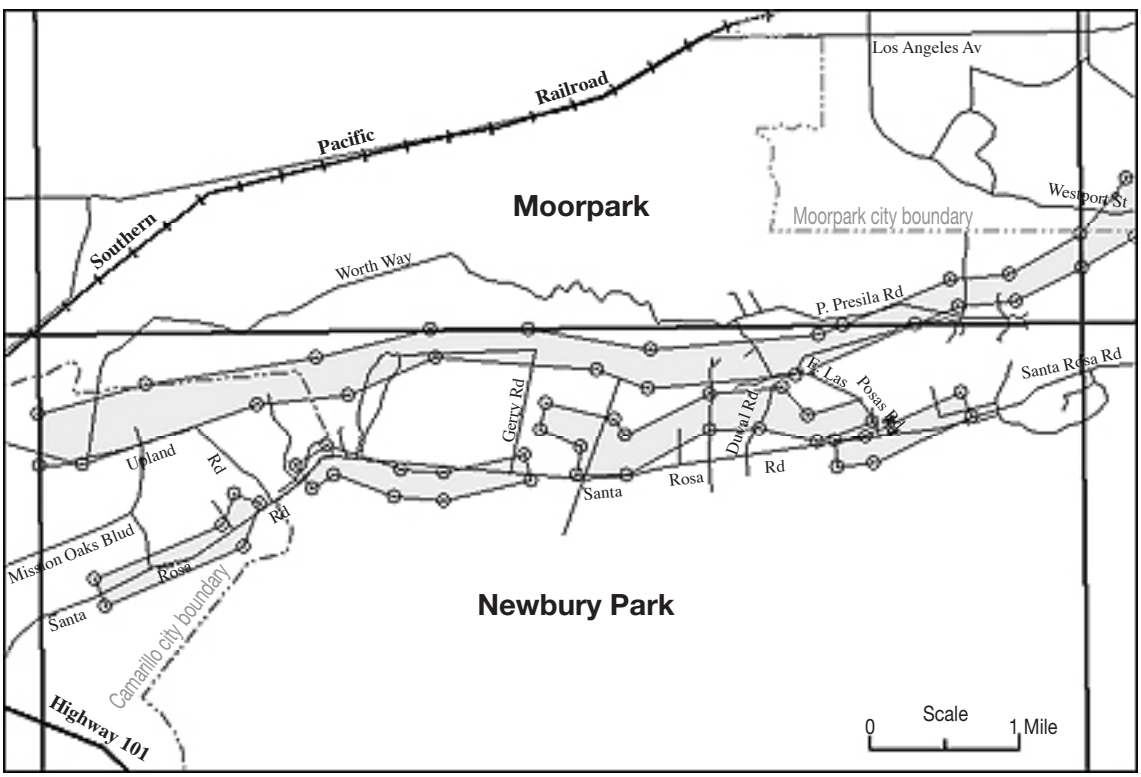

Fig. 17 - Sample Earthquake Fault Zone Map (from: http://www.consrv.ca.gov/dmg/rghm/a-p/releases/mpnp.htm) Official Earthquake Fault Zones (EFZ) encompass traces of the Simi-Santa Rosa fault zone (not shown here). EFZs are shown in yellow; EFZ boundaries are shown as red circles connected by straight red line segments. The city boundary of Camarillo is delineated in light blue and Moorpark is shown in yellow.

5. Conclusions

The higlights of this work are listed below:

1. the strong-motion network on the North Anatolian Fault is very sparse. Denser arrays are necessary in urban areas. The arrays should be supplemented with downhole accelerographs and piezometer arrays in liquefaction susceptible areas. It is important to increase the number of accelerographs in urban environments to cover different geological settings so that the actual motions in the basins and heavily damaged areas can be recorded;
2. detailed site-characterization of the stations are not known. A systematic effort should be embarked upon to characterize the sites;
3. in the event of absence of strong-motion records, aftershock motions have been used to estimate the strong-shaking during the main event. The estimated motions show stronger shaking in the fault-normal direction. Furthermore, on either side of a vertical fault, the

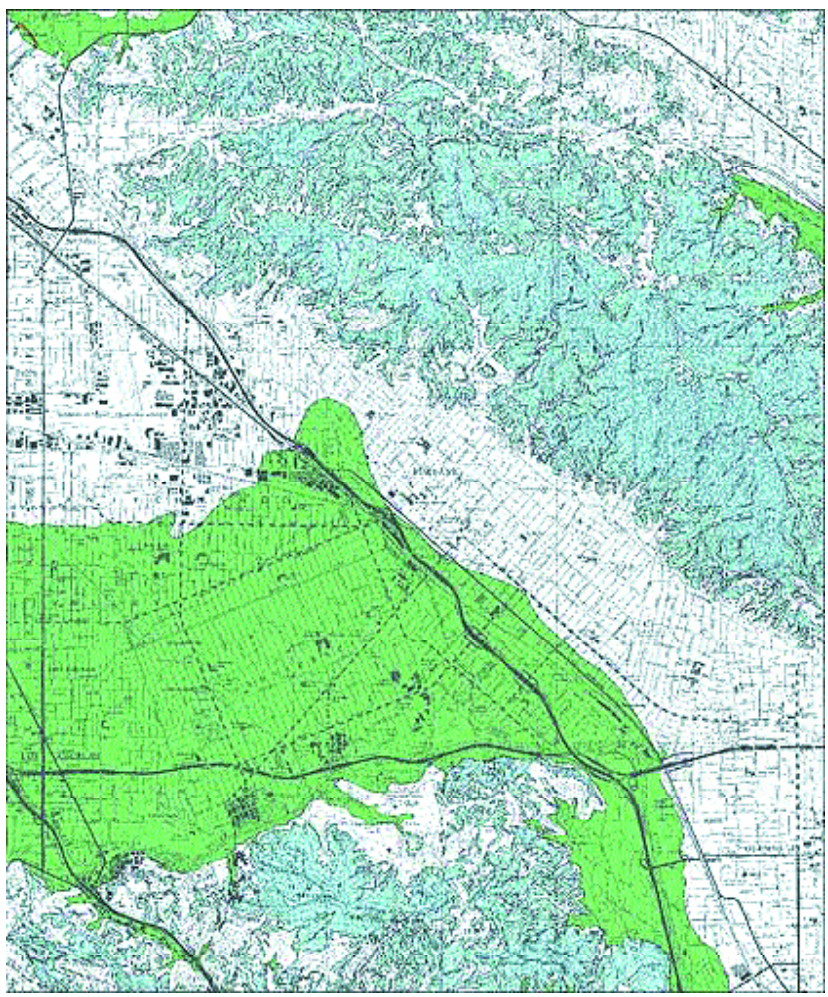

Fig. 18 - A sample hazard map showing liquefaction (green) and landslide (blue) susceptible areas (from HYPERLINK "http://www.consrv.ca.gov/dmg/shezp/maps/m_bur5.htm" http://www.consrv.ca.gov/dmg/shezp/maps/m_bur5.htm).

amplification is proved to be larger on the hanging wall. Therefore, it is essential to better identify existing faults for siting of important infrastructures and facilities;

4. the long-period pulses from near-fault earthquakes must be accounted for in assessing the performance of structures. One possible way is to establish, in selected zones of the NAF, near-fault factors that increase the seismic coefficients in the codes;
5. whenever applicable (e.g. in the Adapazari basin), special site-specific design response spectra should be developed;
6. soil-structure interaction effects possibly adversely affect the performance of the 4-8 story stiff structures (typically reinforced concrete framed buildings with infill walls) in the alluvial basin in Turkey. Most of these buildings have small embedments. Foundations must be properly designed to reduce the adverse effect of such interaction.

Appendix A: Should Turkey establish acts equivalent to Alquist Priolo act of California?

The following are quoted from: HYPERLINK http://www.consrv.ca.gov/dmg/rghm/a-p/releases/mpnp.htm http://www.consrv.ca.gov/dmg/rghm/a-p/releases/mpnp.htm and http://www.consrv.ca.gov/dmg/rghm/a-p/ap-intro.htm

"The Alquist-Priolo Eartrhquake Fault Zoning Act was passed in 1972 to mitigate the hazard of surface faulting to structures for human occupancy. This state law was a direct result of the 1971 San Fernando Earthquake, which was associated with extensive surface fault ruptures that damaged numerous homes, commercial buildings, and other structures. Surface rupture is the most easily avoided seismic hazard".

"The Alquist-Priolo Earthquake Fault Zoning Act's main purpose is to prevent the construction of buildings used for human occupancy on the surface trace of active faults. The Act only addresses the hazard of surface fault rupture and is not directed toward other earthquake hazards. The Seismic Hazards Mapping Act, passed in 1990, addresses non-surface fault rupture earthquake hazards, including liquefaction and seismically induced landslides".

"The law requires the State Geologist to establish regulatory zones (known as Earthquake Fault Zones) around the surface traces of active faults and to issue appropriate maps. ["Earthquake Fault Zones" were called "Special Studies Zones" prior to January 1, 1994.] The maps are distributed to all affected cities, and state agencies for their use in planning and controlling new or renewed construction. Local agencies must regulate most development projects within the zones. Projects include all land divisions and most structures for human occupancy. Single family wood-frame and steel-frame dwellings up to two stories not part of a development of four units or more are exempt. However, local agencies can be more restrictive than state law requires.
Before a project can be permitted, cities and counties must require a geologic investigation to demonstrate that proposed buildings will not be constructed across active faults. An evaluation and written report of a specific site must be prepared by a licensed geologist. If an active fault is found, a structure for human occupancy cannot be placed over the trace of the fault and must be set back from the fault (generally 50 feet)".

References

Abrahamson N.; 2000: Seminar talk at USGS.

Ambraseys N.N.; 1988: *Engineering seismology.* Earthq. Eng. Struct. Dyn., **17**, 1-105.

Aviles J. and Perez-Rocha L.E.; 1998: *Effects of foundation embedment during building-soil interaction*. Earthq. Eng. Struct. Dyn. **27**, 1523-1540.

Barka A.: personal communication, 2000.

Boore D.M.;1983: *Stochastic simulation of high frequency ground motion based on seismological models of radiated spectra*, Bull. Seism. Soc. Am., **73**, 1865-1894.

Boore D.M.; 2001: *Effect of baseline corrections on displacements and response spectra for four recordings of the 1999 Chi-Chi, Taiwan, earthquake,* Bull. Seism. Soc. Am., **91**, 1199-1211.

Çelebi M., Akkar S., Gulerce U., Sanli A., Bundock H. and Salkin A.; 2001: *Main shock and aftershock records of the 1999 Izmit and Duzce, Turkey earthquakes*. USGS-OFR 01-163 (CD-ROM).

Çelebi M. and Sekiguichi H.; 2000: *Estimation of ground motions at Golcuk during the 1999 Kocaeli Turkey earthquake*. AGU Abstract, San Francisco, Ca. Dec. 2000.

Çelebi M. and Sekiguichi H.; 2001: *Estimation of ground motions at Golcuk during the 1999 Kocaeli Turkey earthquake*. In preparation.

Irikura K.; 1986: *Prediction of strong acceleration motion using empirical Green's function,* Proc. 7th Japan Earthq. Symp., 151-156.

Lee W., Shin T., Kuo K. and Chen K.; 1999: *CWB free-field strong-motion data from the 9-21-1999 Chi-Chi earthquake*. Volume 1: Digital Acceleration Files on CD-ROM, Pre-Publication version (December 6, 1999). Seismology Center, Central Weather Bureau, Taipei, Taiwan.

Nakamura Y.; 1989: *A Method for Dynamic characteristics estimation of subsurface using microtremor on the ground surface*. Quart. Rep. Railway Tech. Res. Inst. (RTRI), **30**, 25-33.

Nakamura Y.; 2000: *Clear identification of fundamental idea of Nakamura's technique and its applications,* Proc., 12th World Conf. Earthq. Eng. Auckland, New Zealand (CD-ROM).

Novikava E.I. and Trifunac M.D.; 1994: *Duration of ground motion in terms of earthquake magnitude, epicentral distance, site conditions and site geometry.* Earthq. Eng. Struct. Dyn., **23**, 1023-1043.

Parsons T., Toda S., Stein R., Barka A. and Dieterich J.; 2000: *Heightened odds of large earthquakes near Istanbul: An interaction-based probability calculation*. Science, **288**, 661-665.

Sekiguchi H. and Iwata T.; 2000: *Rupture process of the 1999 Kocaeli, Turkey, earthquake estimated from strong-motion waveforms*. Bull. Seism. Soc. Am., **92**, 300-311.

Sieh K.: Personal communication, 2000.

Somerville P.; 1998: *Development of an improved representation of near-fault ground motions, SMIP98 Seminar on Utilization of Strong-Motion Data*. Dept. of Conservation, Div. of Mines and Geology, Calif. Strong Motion Instrumentation Program, Sept. 15, 1998.

Somerville P.G., Irikura K., Graves R., Sawada S., Wald D.J., Abrahamson N., Iwasaki Y., Kagawa T., Smith N. and Kowada A.; 1999: *Characterizing crustal earthquake slip models for the prediction of strong ground motion*. Seism. Res. Lett., **70**, 59-80.

Ministry of Public Works and Settlement Government of Republic of Turkey; 1998. *Specification for structures to be built in disaster areas*. Issued on: 2.9.1997, Official Gazette No. 23098. Effective from: 1.1.1998, Amended on: 2.7.1998, Official Gazette No.23390 (English translation by N. Aydinoglu, 1998).

Tsai Y-B: (no date): *Some observations about the Chi-Chi, Taiwan earthquake of September 21, 1999*. Technical Report, National Taiwan University (Taiwan), 29 pp.

U. S. Geological Survey; 2000: *Implications for earthquake risk reduction in the United States from the Kocaeli, Turkey, earthquake of August 17, 1999*: U.S. Geological Circular 1193, 64 pp.

Uniform Building Code; 1997: *International Conference of Building Officials*. Whittier, Ca.